

Article

Estimating Calorific Value of Coal Using Laser-Induced Breakdown Spectroscopy through Statistical Algorithms: Correlation Analysis, Partial Least Squares, and Signal-to-Noise Ratio

Soo-Min Kim ^{1,2}, Kyung-Hoon Park ^{1,3}, Choong-Mo Ryu ¹, Jung-Hyun Choi ⁴  and Seung-Jae Moon ^{1,*} ¹ Department of Mechanical Convergence Engineering, Hanyang University, Seoul 04763, Korea² Korea Authority of Land and Infrastructure Safety, Jinju 52852, Korea³ Korea Automotive Technology Institute, Cheonan 31214, Korea⁴ Department of Environmental Science and Engineering, Ewha Womans University, Seoul 03760, Korea

* Correspondence: smoon@hanyang.ac.kr

Featured Application: This work can be applied to in situ estimation measurements of the calorific value of coal using laser-induced breakdown spectroscopy.

Abstract: The objective of this study was to compare different statistical algorithms for estimating the calorific value of coal based on a quantitative analysis of the elements in coal. Laser-induced breakdown spectroscopy (LIBS) was applied for the elemental analysis. Three different algorithms, including the correlation analysis (CA) method, the partial least squares (PLS) analysis method, and the signal-to-noise ratio (SNR), were adopted to accurately determine the concentrations of the elements in coal by using Dulong's equation. Special emphasis was placed on the selection of the delay time to improve the measurement accuracy. The coefficient of determination, R^2 , was considered for optimizing the delay time. The intensity–concentration calibration curves were obtained for the elements in coal and the elemental concentration correlations were estimated on the basis of the calibration curves of each element. The CA showed a higher accuracy compared to PLS and the SNR. This confirmed that LIBS shows potential for the rapid determination of the calorific value of coal.

Keywords: laser-induced breakdown spectroscopy; correlation analysis; partial least squares; signal-to-noise; calorific value; delay time



Citation: Kim, S.-M.; Park, K.-H.; Ryu, C.-M.; Choi, J.-H.; Moon, S.-J. Estimating Calorific Value of Coal Using Laser-Induced Breakdown Spectroscopy through Statistical Algorithms: Correlation Analysis, Partial Least Squares, and Signal-to-Noise Ratio. *Appl. Sci.* **2022**, *12*, 11517. <https://doi.org/10.3390/app122211517>

Academic Editor: Saulius Juodkazis

Received: 12 October 2022

Accepted: 8 November 2022

Published: 13 November 2022

Publisher's Note: MDPI stays neutral with regard to jurisdictional claims in published maps and institutional affiliations.



Copyright: © 2022 by the authors. Licensee MDPI, Basel, Switzerland. This article is an open access article distributed under the terms and conditions of the Creative Commons Attribution (CC BY) license (<https://creativecommons.org/licenses/by/4.0/>).

1. Introduction

Coal is the primary fuel of power plants in Korea, and coal-fired power plants have produced around 40% of the country's total electricity in recent years. In a coal-fired power plant, measuring the calorific value is important for the plant's efficiency and its environmental impact, since information on the coal components can be valuable for supplying the appropriate amount of excess combustion air. For given operating conditions, the supply of coal for a known calorific value is important for estimating the power plant's efficiency. Therefore, the development of a real-time measurement technique to analyze the calorific value of coal is required. Laser-induced breakdown spectroscopy (LIBS) is an in situ measurement that detects the elemental composition from the specific wavelengths of each element [1–4]. LIBS can be used for analyzing solid [5], liquid [6], and gas [7] samples within the detection limits of specific ppm levels. Conventionally, the loss on ignition method and a CHN (carbon, hydrogen, and nitrogen) analyzer have been used for determining the coal components.

In the aforementioned methods, the coal samples must be pre-treated and the analysis takes more than 10 h. On the contrary, LIBS needs little or no sample preparation compared to the conventional loss on ignition method and less time to analyze the result. In LIBS,

the intensity of the signal depends on the concentration of the elemental components. The signal intensity shows a transient evolution behavior after laser pulse irradiation. To increase the measurement accuracy, the appropriate detection time, which is controlled by a delay time, should be determined [8–10].

To increase the accuracy of component analyses for various types of samples, studies on the effects of variation in the experimental parameters have been carried out [11,12]. Li et al. [13] investigated the variables that affect the precision of LIBS measurements for pelletized coal samples. The experimental parameters, including the relative standard deviation, the pressure to pelletize the coal sample, deviations from the focal point of the sample, the number of laser shots, and various ambient gases, were investigated. Sivakumar et al. [14] experimentally and numerically presented the effect of the packing density of pellets on the fluctuation of emission lines in C and Fe. A numerical model based on the two-dimensional random close packing of disks in a confined geometry showed a good agreement with the experimental results. The results showed that finer particles in a binary sample provided a higher homogeneity in the laser–target interaction region, which yielded smaller fluctuations in the LIBS emission lines. Besides improving sample preparation, statistical approaches have been applied to data processing to improve the estimation accuracy. Feng et al. [15] derived the coefficients of determination, R^2 , based on a partial least squares regression analysis and presented a method for determining the concentration of coal by using a function with the correction factor of a simple regression analysis. In their work, a total of 40 laser spectra were used to increase the accuracy of measurements of the carbon and hydrogen contained in bituminous coal. Using the partial least squares method, they derived the coefficient of determination ($R^2 = 0.880$). Using the root mean square error of prediction (RMSEP) in a simple regression analysis, the error was reduced to a range from 4.47 to 5.52%. Li et al. [16] investigated the influences of different spectral preprocessing methods such as smoothing, standard normal variate transformation, multiplicative scatter correction, mean centering, and derivation by convolution (the Savitzky–Golay method) on a quantitative model for the calorific value analysis of coal. Ismail et al. [12] and Lee et al. [17] used the signal-to-noise ratio (SNR) for the selection of the delay time. By measuring a total of 25 points, the impact of laser energy on the SNR was analyzed. The delay time generating the highest SNR value was selected as the optimal delay time. However, the SNR method needs a reference signal without any background noise. The SNR value varies significantly according to the value of the noise. The width of the signal intensity requires a correction because these values may change with the movement error of the measurement.

In this study, the appropriate delay time was selected based on an estimation of the calorific values obtained from three different data analytical methods, including correlation analysis (CA), the partial least squares (PLS), and the SNR methods. At the determined delay time, the LIBS intensity signals were collected and the calorific value was estimated with the intensity data via the CA, PLS, and SNR methods. The coefficient of determination (R^2) was considered to evaluate the measurement accuracy of each analysis method. The obtained calorific values of the coal samples were compared to those of the chemical analysis method to assess the accuracy of the analysis methods.

2. Experiments

2.1. Experimental Setup

As shown in Figure 1, the LIBS system is composed of two main parts, which are the laser generation part, Figure 1a, and the signal collection part, Figure 1b [18]. In the laser generation part, the laser pulse was focused to ablate the target sample, and the plasma was then induced from the ablated sample. The laser source was an Nd-YAG (Litron Lasers Inc., Rugby, UK) operating at a wavelength of 1064 nm and an energy of 30 mJ over a pulse duration of 8 ns with a repetition rate of 1 Hz in Q-switch mode. A 100 mm focal length lens (Thorlabs Inc., Newton, NJ, USA) was used to focus the beam onto the sample surface. In the signal collection part, the spectrometer collected the emitted signals when

the excited electrons from atoms and ions came back to the ground state. The light from the induced plasma was focused through a plano-convex lens with a 40 mm focal length lens to a fiber-optic bundle. A fiber-optic cable with a 1 mm diameter was installed at an angle of 45° with respect to the normal direction of the sample surface. The optical fiber was directly connected to the slit entrance of a spectrometer with four-channel charge-coupled devices (J200, Applied Spectra, Fremont, CA, USA). The spectrometer had a spectral range of 180–884, a spectral resolution of 0.1 nm, and a signal-to-noise ratio of about 250:1. A digital delay/pulse generator (Stanford Research Systems, model DG535) was used to control the delay times when the data were recorded. The software program Aurora was used for data acquisition. The integration time was set at 1.05 ms [19].

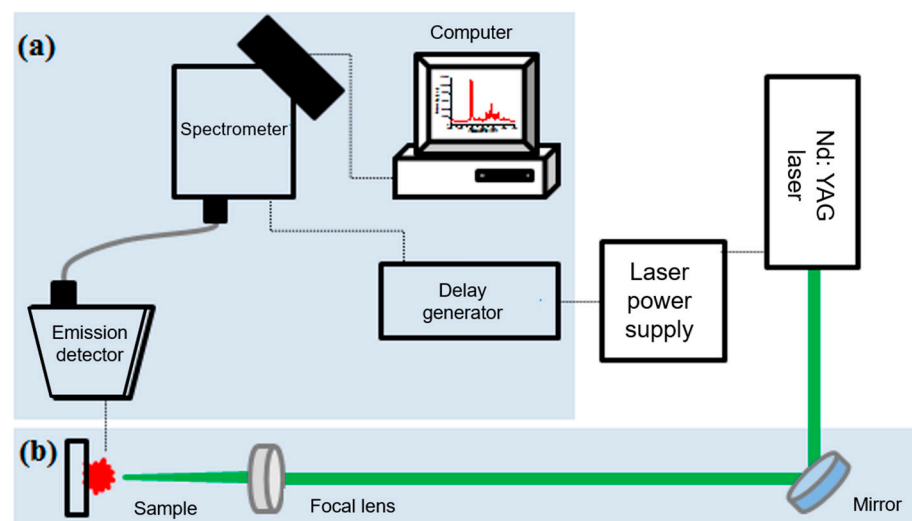


Figure 1. Schematic diagram of LIBS device; (a) spectrometer and (b) optics.

2.2. Sample Preparation

Seven different bituminous coal samples that were actually used in a coal-fired power plant in Korea were prepared. For the reference data, the elemental concentration was determined from the conventional industrial chemical analysis. The concentrations of carbon, hydrogen, and nitrogen were determined by a C/H/N elemental analyzer (5E Series, Daeduck Analytical Research Institute). The concentration of the sulfur was measured via a 5E-S3200 Coulomb sulfur analyzer. The concentration of oxygen was calculated by subtracting the concentration of the remaining elements and the concentration of ash from 100%.

The elemental concentrations of each coal sample are shown in Table 1. The method that is widely practiced to evaluate the higher heating value (HHV) of coal, which is known as the calorific value, is by using Dulong's equation. Dulong's equation uses the weight fractions of carbon, hydrogen, oxygen, and sulfur to predict the higher heating value. Dulong's equation is as follows [20]:

$$HHV(\text{kcal/kg}) = 8080C + 34460\left(H - \frac{O}{8}\right) + 2250S \quad (1)$$

where C , H , O , and S are the concentrations of carbon, hydrogen, oxygen, and sulfur, respectively. Therefore, we presented 4 main components to obtain the calorific value in Table 1. From Equation (1), the higher heating value of coal is a positive function of the carbon, hydrogen, and sulfur concentrations. From Table 1, the coal samples were mainly composed of about 65 to 75% carbon. Carbon and hydrogen are the dominant components used to evaluate the calorific value.

Table 1. Description of coal sample.

Coal Name	Concentration (wt%)			
	C	H	O	S
GUNVOR	74.4	5.21	12.46	0.71
MSJ-1	69.8	5.16	16.20	0.93
MSJ-2	67.5	5.27	17.27	0.84
LANNA HARITA	68.3	5.08	18.03	0.53
MACQUARIE	67.5	4.81	18.27	1.10
PEABODY	66.3	5.01	17.96	0.67
KPU	65.6	5.25	20.97	0.10

The coal samples were initially pulverized into a powder form. By using a scale (HR-250A), 0.3 g of each coal sample was prepared and pelletized into a 13 mm-diameter and a 2 mm-thickness under a pressure of 10 tons using a hydraulic press (PN 181-1110) as shown in Figure 2 (left). To improve the measurement accuracy of the samples, 100 points (10 × 10) were measured for each delay time from 0.2 to 2 μs by 0.2 μs, as shown in Figure 2 (right).

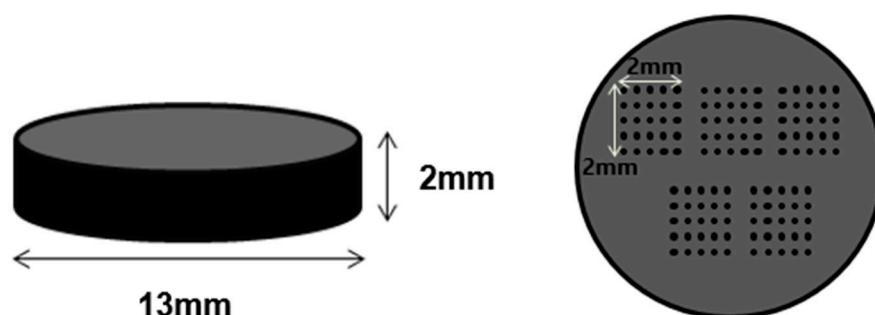


Figure 2. Pellet sample of pulverized coal.

3. Theory

3.1. Grubbs Test

The coefficient of determination, R^2 , and the error vary according to the number of measured points. As the number of measured points increases, the coefficient of determination value tends to become closer to 1 and the error decreases. In Figure 3, the coefficient of determination was above 0.9 from 48 points at a wavelength of 247 nm in C. When the coefficient of determination is above 0.9, the reliability of the data can be considered to be high. To eliminate the suspicious data, the maximum and minimum values were subjected to Grubbs test to determine whether the value was an outlier.

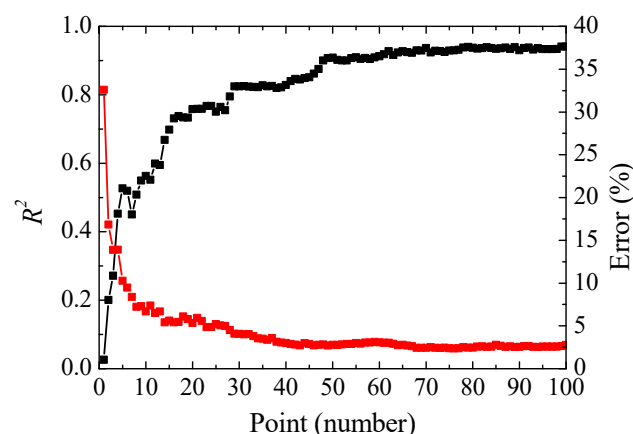


Figure 3. Variation in coefficient of determination and error.

From Equation (1), the average of the signal intensities of the carbon for each value of G in the data was calculated from 1.75 to 3.19. For the 100 measurement points, the critical

values of G were 3.38 and 3.21 at the confidence levels of 95 and 97.5%, respectively [21]. The maximum G value, 3.19, satisfied the above criterion at the confidence levels of 95 and 97.5%:

$$G = \frac{|\bar{X}_{\max,\min} - \bar{X}|}{s} \tag{2}$$

where s , \bar{X} , and $\bar{X}_{\max,\min}$ are the standard deviation, sample mean value, and sample maximum or minimum value, respectively.

3.2. Partial Least Squares

The partial least squares (PLS) method is considered as a good alternative to principal component regression (PCR). The PLS method is a more robust approach when the data are analyzed by a regression for the independent variables X and the dependent variables Y . The PLS is built with a set of outer relations that describe X or Y as linear combinations of components, as presented in Equation (2) [22]. The quality of a PLS model can be evaluated by the coefficient of determination, R^2 , which provides information about the variation in the used data sets. One variable is assumed to be the explanatory variable, and the other variable is assumed to be a response variable. The coefficient of determination represents the quality of the data adjustment within a straight line, and the value is 1 when there is total agreement between the real and estimated values [23,24].

$$X = TP' + E = \sum_{h=1}^H t_h p'_h + E, \tag{3}$$

$$Y = UQ' + F = \sum_{h=1}^H u_h q'_h + F \tag{4}$$

where T and U are the score matrices, P' and Q' are the loading matrices of X and Y , respectively, and E and F are the residuals of X and Y .

3.3. Signal-to-Noise Ratio

In the signal-to-noise ratio, the integrated peak area of the target element is divided by the root mean square noise multiplied by the peak widths. The integrated peak area of the target element's emission line, the peak width, and the root mean square (RMS) noise are acquired from the spectral emission lines. The RMS noise is obtained from the baseline intensities, which are adjacent to the element emission lines [25].

$$SNR = \frac{(\text{Integrated peak area})}{(\text{RMS noise})(\text{Peak width})} \tag{5}$$

3.4. Correlation Analysis

A correlation analysis (CA) measures the association between variables with the linear correlation coefficient, R , and the correlation coefficient can be expressed in the following form [26]:

$$R = \frac{\sum_i (x_i - \bar{x})(y_i - \bar{y})}{\sqrt{\sum_i (x_i - \bar{x})^2} \sqrt{\sum_i (y_i - \bar{y})^2}} \tag{6}$$

where \bar{x} and \bar{y} are the means of x_i and y_i , respectively.

R ranges from -1 to 1 . $R = 1$ corresponds to the perfect positive correlation when the points are in same straight line with a positive slope. The coefficient of determination, R^2 , is used to assess the reliability of a linear relationship between x (intensity measured for the sample) and y (intensity measured for other samples).

4. Results and Discussion

Selecting the delay time during an LIBS analysis is an important part of measuring elements. The intensity of the signal is greatly affected by the delay time. Generally, the delay times for detecting the emission signal of an ablated sample is under 100 ns for continuum emission, 500 ns–20 μ s for atomic emission, and 100 ns–5 μ s for ionic emission. At the continuum emission, the time for excited atoms to come back to the ground state is too short to be detected. Since the spectral emission lines are eventually extinguished, the time for capturing the signals is important to improve the measurement accuracy. The appropriate delay times are known to vary with the transformation of the ion and the elemental composition of the sample [8–10]. The appropriate delay time for a quantitative analysis of a target sample is determined by the coefficient of determination, R^2 .

In Figure 4, coefficients of determination, R^2 with various delay times are presented to determine the appropriate delay time for the quantitative analysis of coal samples. The spectrometer delay time varied from 0.2 to 2.0 μ s by a 0.2 μ s interval. The 100 spectra samples were consecutively captured at each delay time. The calibration curves for the 100 spectra were obtained using the CA, PLS, and SNR methods. From the calibration curves, the R^2 were calculated for delay times from 0.2 to 2.0 μ s. The R^2 with the CA showed a relatively high value compared to those of the other analysis methods. The highest R^2 for a 1.4 μ s delay time for the CA and PLS methods were 0.97 and 0.91, respectively. However, the highest R^2 of the signal-to-noise ratio method for a 1.0 μ s delay time was 0.77.

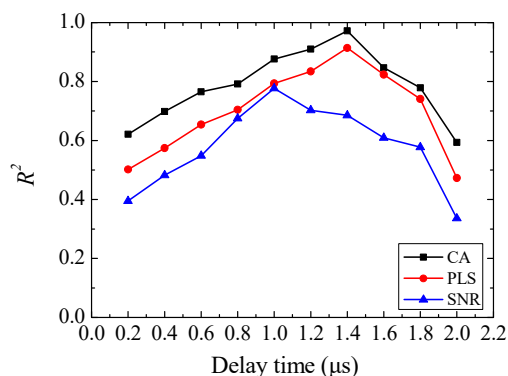


Figure 4. The coefficients of determination, R^2 with various delay times for the CA, PLS, and SNR methods.

Figure 5 shows the seven emission spectra for seven coal samples at 247.7 nm for C, 656.2 nm for H, 844.6 nm for O, and 544.65 nm for S. All four emission lines were clearly identified from adjacent emission lines, and they were obtained with a delay time of 1.4 μ s. The wavelengths of 247.7, 656.2, 844.6, and 544.65 nm are known to be characteristic wavelengths for identifying the existence of carbon, hydrogen, oxygen, and sulfur, respectively, in coal samples. In Figure 5a, the carbon emission spectrum for Gunvor presented the maximum intensity due to the highest C concentration (74.4%) among the seven coal samples, as shown in Table 2. In Figure 5b, the highest hydrogen emission spectrum appears to occur in the Gunvor sample. However, the base signal line for the Gunvor sample is shifted a little bit. Considering this, the magnitude of the hydrogen spectra for the seven samples is almost identical. Compared to other components such as hydrogen and sulfur, the maximum intensity of the carbon spectrum was much higher than those of the other components. In Figure 5e, the average value of 100 spectra from the seven different coal samples is shown as a full spectrum obtained from the spectrometer.

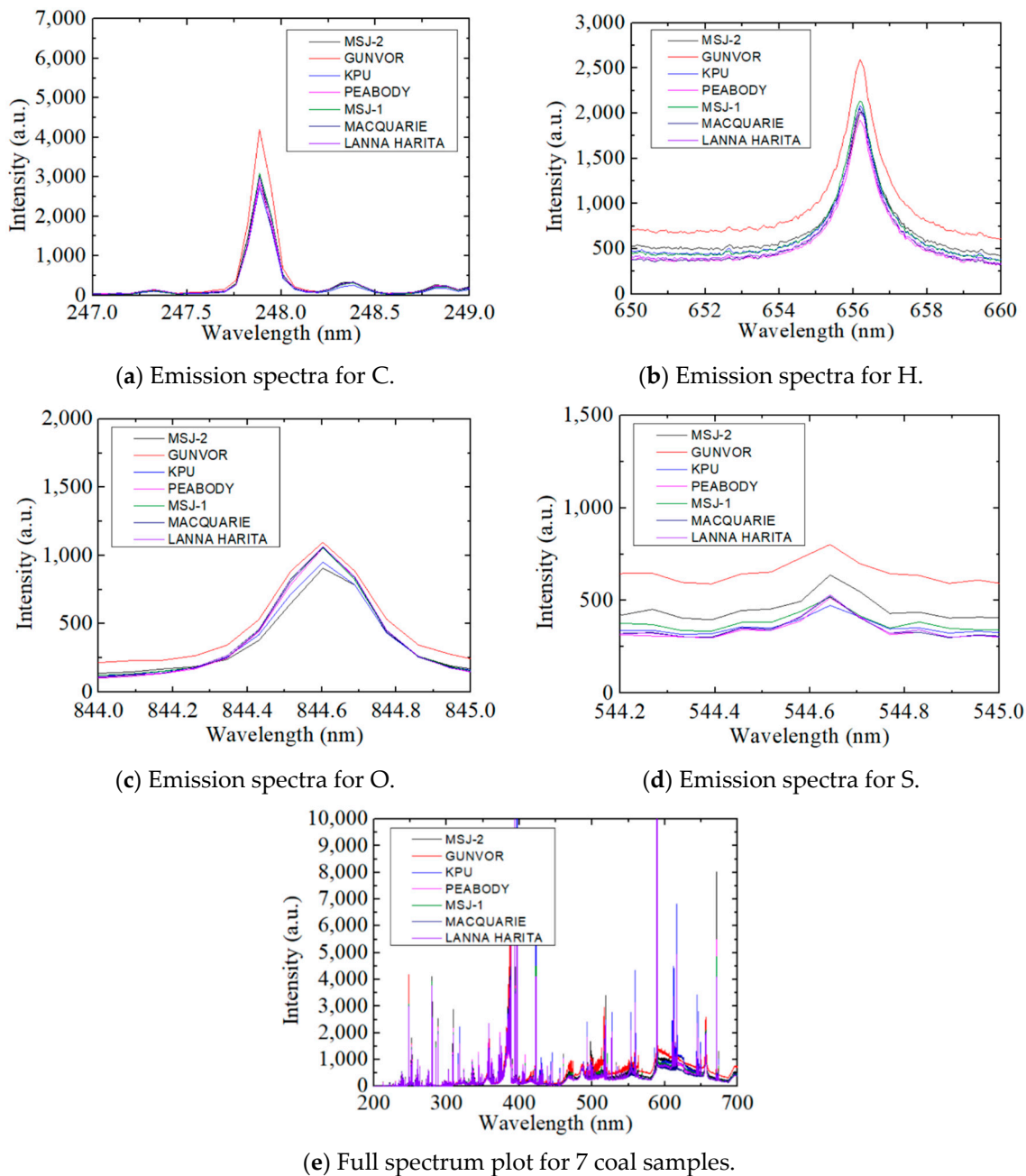


Figure 5. Sample emission spectra for (a) carbon, (b) hydrogen, (c) oxygen, (d) sulfur, and (e) full spectrum plot for seven coal samples.

Table 2. Predicted calorific value of various coal samples by correlation analysis.

Coal Name	Concentration (%)				Calorific Value (kcal/kg)	Chemical Analysis (kcal/kg)	Error
	C	H	O	S			
GUNVOR	75.03	5.27	12.55	0.46	7348.22	7360	0.16
MSJ-1	68.7	5.21	13.88	0.52	6760.15	6915	2.24
MSJ-2	68.1	5.15	17.96	0.84	6522.44	6852	4.81
LANNA HARITA	67.55	5.01	18.23	0.72	6415.43	6619	3.08
MACQUARIE	67.32	4.48	17.43	0.64	6246.87	6705	6.83
PEABODY	66.3	4.77	18.03	0.58	6237.19	6630	5.92
KPU	64.18	4.08	10.46	0.67	6156.22	6619	6.99

In Figure 6, the correlation between the intensity of the LIBS signal at 247.7 nm and the concentration of carbon in coal samples was analyzed with delay times of 1.4 μs for the CA and PLS methods and 1.0 μs for the SNR method. The signal intensity at a wavelength of 247 nm, which is a representative spectrum of the atomic carbon from the LIBS spectra data, was selected for estimating the carbon concentration in the samples. Because the used coal samples were composed of over 60% carbon, the intensity of the carbon signal was larger than those of the other remaining elements. The carbon signal could be easily distinguished from the other elements. Depending on the coal sample, the carbon concentration varied from about 65 to 75% and the signal intensities were proportional to the carbon concentration. The R^2 for the CA, PLS, and SNR methods was 0.98, 0.92, and 0.65, respectively. The magnitude of the error bars in the carbon samples were relatively small compared to that of the other elements, with a maximum of 4.3, 5.1, and 5.7% from the mean value for the CA, PLS, and SNR methods, respectively. This was caused by the large quantity of carbon in the coal samples.

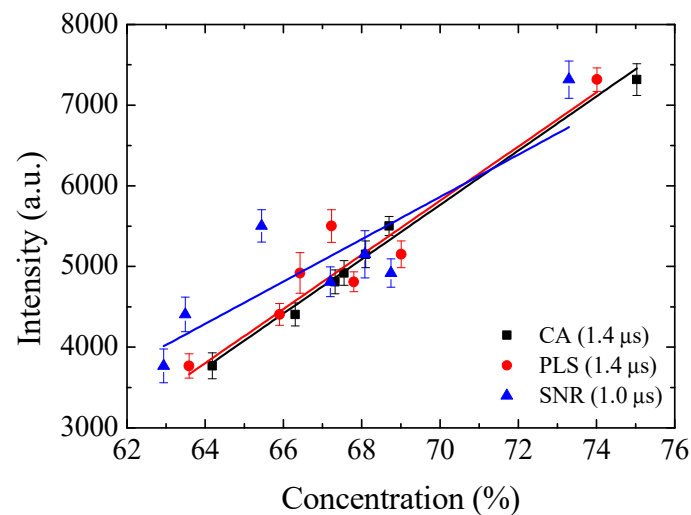


Figure 6. Correlation between the intensity and C concentration with maximum R^2 for CA, PLS, and SNR methods.

In Figure 7, the correlation between the LIBS signal intensity and the hydrogen concentration in coal was analyzed at the wavelength of 656.2 nm in the LIBS spectrum. The R^2 for the CA, PLS, and SNR methods was 0.13, 0.14, and 0.06, respectively. The error bars represent the standard deviation of the signal intensity from the average intensity of 100 points. The standard deviation of the hydrogen peak was larger than that of carbon peak, as shown in Figure 6, which showed 7.7, 13.9, and 14.2% of maximum errors from the mean values for the CA, PLS, and SNR methods, respectively. The hydrogen concentrations in the coal samples ranged between 4.8 and 5.2%. The low concentration gave a low signal intensity and a small variation of less than 0.5% in hydrogen between the samples produced difficulty in distinguishing the intensity variation to identify the hydrogen concentration.

In Figure 8, the LIBS signal intensity at the 844.6 nm wavelength was calibrated with the oxygen concentration in the coal samples. The oxygen concentration in the coal samples was found to be between 12 and 20% from Table 1. Oxygen is the second most abundant element in coal. The difference between the oxygen concentrations of different samples, which was relatively large compared to that of hydrogen, gave a better R^2 value for the CA, PLS, and SNR methods, with values of 0.15, 0.18, and 0.16, respectively. In addition, as the LIBS signal was collected under atmospheric conditions, the oxygen in the atmosphere affected the measurement accuracy of the oxygen in coal. This resulted in a larger maximum errors compared to that of hydrogen, with values of 15.7, 26.8, and 27.4% for the CA, PLS, and SNR methods, respectively.

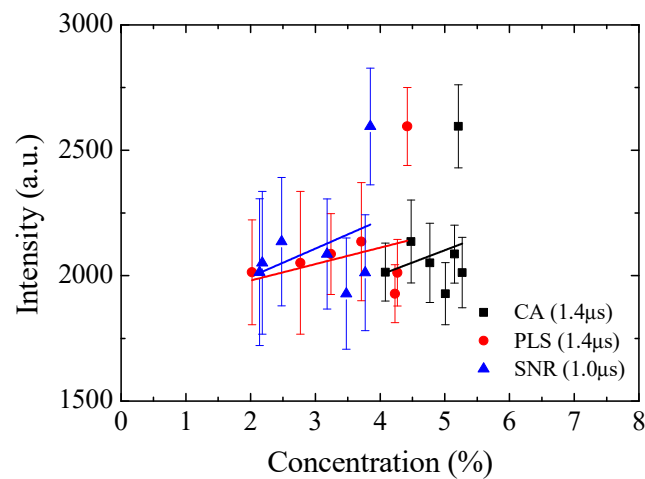


Figure 7. Correlation between the intensity and H concentration with maximum R^2 for CA, PLS, and SNR.

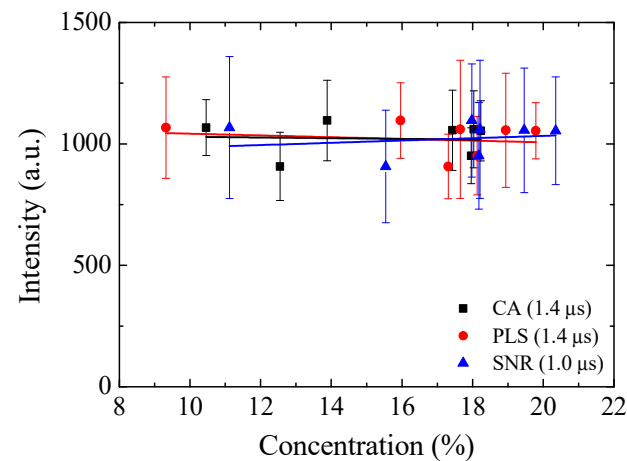


Figure 8. Correlation between the intensity and O concentration with maximum R^2 for CA, PLS, and SNR methods.

In Figure 9, the LIBS signal intensity at the wavelength of 544.65 nm was calibrated with the sulfur concentration in the coal samples. The sulfur concentration in coal varied from 0.5 to 1.1%, as shown in Table 1. The overall peak intensity of sulfur was quite similar to that of oxygen, as shown in Figure 7. In spite of the small variation in the sulfur concentrations, the sulfur showed a better peak intensity variation and smaller error bars compared to oxygen, which allowed for a better estimation of the sulfur concentration. The R^2 for the CA, PLS, and SNR methods was 0.98, 0.65, and 0.02, respectively. The maximum errors from the mean values were 17.2, 17.9, and 16.3% for the CA, PLS, and SNR methods, respectively. In the CA and PLS analyses, the signal intensity increased with an increase in the sulfur concentration. In the SNR method, the signal intensity showed the opposite trend. Because the SNR method considers both the peak intensity and the baseline noise, the increased baseline noise at higher sulfur concentrations could result in the opposite trend with other methods.

The most significant factor in increasing the LIBS measurement error was the noise, which was greater than the signal of the element. The degree of homogenization of the sample, the laser output, and interference of the plasma spectrum with the emissions from the element are associated with noise. For a more accurate analysis, it is possible to minimize the noise by reducing the background of the spectrum.

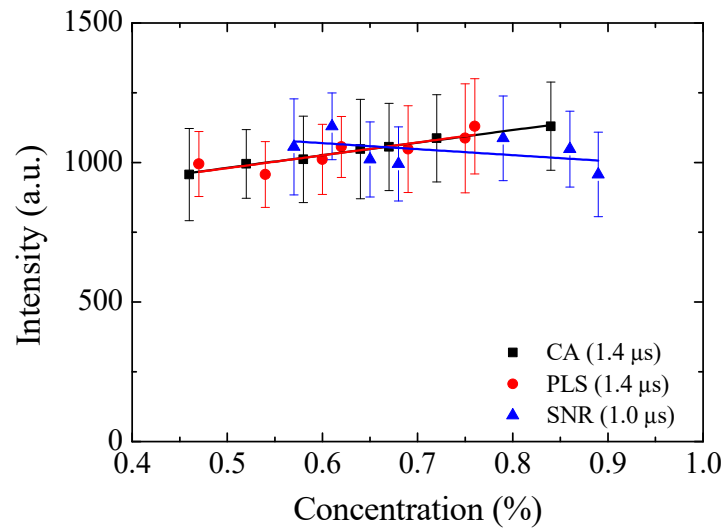


Figure 9. Correlation between the intensity and S concentration with maximum R^2 for CA, PLS, and SNR methods.

Figure 10 shows the relationship between the carbon concentration of a coal sample used for an LIBS measurement and the estimated concentration of the carbon that is obtained from the CA, PLS, and SNR methods with the signal intensity of the target elements from the LIBS spectrum. The dotted line in Figure 9 presents the points where the estimated concentration of the element was equal to the measured concentration in the coal sample. When the mark is closer to the dotted line, the estimation of the elemental concentration of the coal sample is better. In Figure 10, the estimated concentration of carbon from the CA shows a better accuracy compared to other analysis methods. A clear distinction among the signal intensities of carbon for different concentrations in the coal samples could increase the accuracy of the estimation of the carbon content.

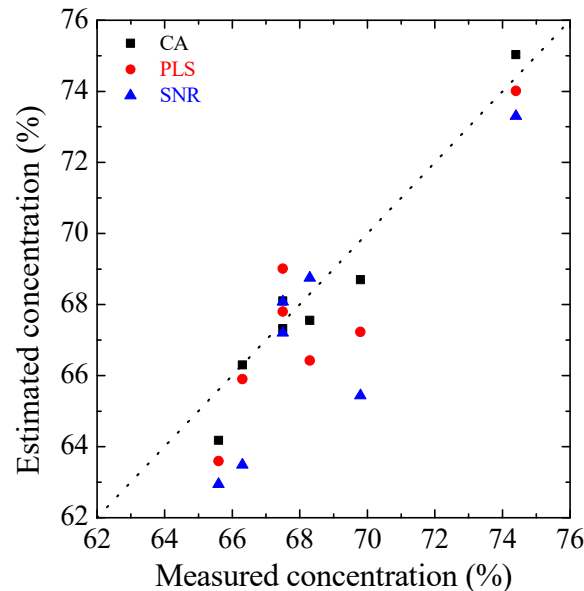


Figure 10. Estimated carbon concentrations with CA, PLS, and SNR.

In Figure 11, the relationship between the estimated concentration of hydrogen using the LIBS signal intensity and the known concentration of hydrogen in the coal sample is depicted. As shown in Table 1, the hydrogen concentration in the coal sample was between 4.8 and 5.2%. The LIBS signal peak intensity difference with changes in the concentration of hydrogen in the sample may not be clear, and this affects the estimation

accuracy. The peak intensity itself was small when the concentration of the target element in the sample was small. This increased the effects of the baseline noise. For that reason, the estimation accuracy for the hydrogen concentration using the PLS and SNR methods was low compared to that of the CA method. Overall, the hydrogen concentration in the coal sample was underestimated.

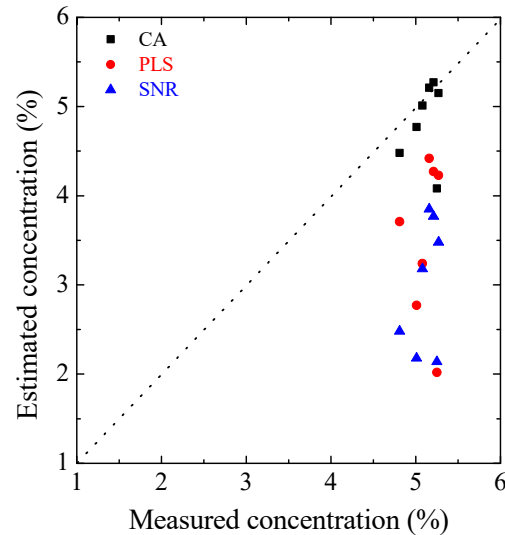


Figure 11. Estimated hydrogen concentration with CA, PLS, and SNR.

In Figure 12, the relationship between the estimated concentration of oxygen using the LIBS intensity and the known concentration of oxygen in the coal sample is presented. Because the experiment was performed under atmospheric conditions, the oxygen content in the atmosphere affected the LIBS signal intensity for the oxygen measurement. Unlike the other elements under consideration, more than half of the marks located on the upper side of the diagonal line represent the tendency for overestimating the oxygen content. The KPU sample from Table 1 consisted of 20.97% oxygen, which is similar to the oxygen content in the air and shows a low estimation accuracy. The CA performed on the other samples showed estimated concentrations of oxygen that were close to the diagonal dotted line.

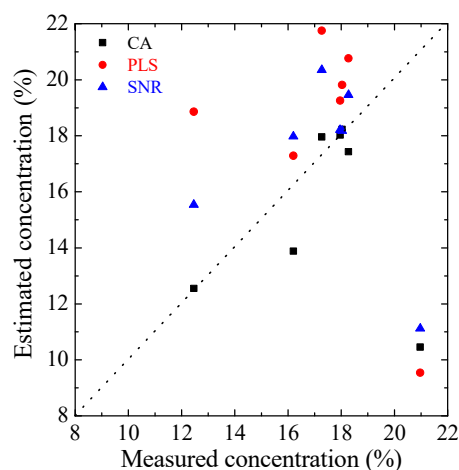


Figure 12. Estimated oxygen concentrations with CA, PLS, and SNR.

In Figure 13, the sulfur concentrations in the coal sample as estimated from the LIBS intensity were compared with the known concentration of sulfur in the sample. The sulfur concentration was approximately 1% in the coal sample. The sulfur peak from the LIBS spectrum could be identified in spite of the small concentration. The intensity of the peak was quite similar to that of the baseline noise. This could lead to the peak intensity fluctuations being affected by the baseline noise intensity fluctuations.

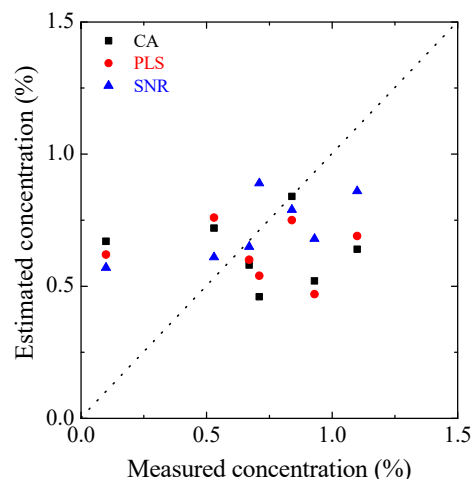


Figure 13. Estimated sulfur concentration with CA, PLS, and SNR.

In this study, LIBS was performed in the air. Errors due to the gas components in the air may affect the measurement of elements, especially O and H. However, the CA method showed an improved accuracy with a coefficient of determination of 0.971 compared to the PLS and SNR methods with the R^2 s of 0.914 and 0.777, respectively. The CA method showed the negligible measurement error in the air.

In Table 2, the estimated concentrations of the target elements in the coal sample to calculate the calorific value of coal are presented. The calorific values were calculated with Dulong's equation based on the estimated concentrations of the elements in coal using the LIBS signal intensity with the CA method. The calculated calorific value was compared to the calorific value obtained from a bomb calorimeter presented as a chemical analysis. The error between the calculated calorific value and the calorific value from the chemical analysis was from 0.16 to 6.99%. By comparing Tables 1 and 2, the percent difference between the estimated concentrations of the elements in the coal samples and the known concentrations could be determined. From Equation (1), the accuracy of the calorific value calculation of coal is most affected by the percent difference in the estimated concentration of hydrogen, because hydrogen has the biggest coefficient value. With a similar magnitude of the percent difference in the estimated concentration, hydrogen brought about a bigger error in the calorific value estimation than carbon.

In Table 3, the estimated concentrations of the elements in coal using the LIBS signal intensity with the PLS method is shown. The error between the calorific values calculated using Dulong's equation and the chemical analysis was found to be from 8.72 to 17.71%. The estimated carbon concentration had around a 2% difference from the sample's carbon concentration, which is a similar level of accuracy as with the CA. As shown in Figure 11, the PLS method had a low accuracy in predicting the hydrogen concentration in coal compared to the CA method. It showed a maximum error of a 3% difference from the sample. The underestimated hydrogen concentration made the percent error bigger in the calorific value calculation.

Table 3. Predicted calorific value of various coal samples by partial least squares.

Coal Name	Concentration (%)				Calorific Value (kcal/kg)	Chemical Analysis (kcal/kg)	Error
	C	H	O	S			
GUNVOR	74.01	4.27	17.31	0.54	6717.97	7360	8.72
MSJ-1	67.23	4.42	15.96	0.47	6278.41	6915	9.21
MSJ-2	66.42	4.23	19.79	0.75	5988.81	6852	12.60
LANNA HARITA	69.01	3.24	18.13	0.76	5928.66	6619	10.43
MACQUARIE	67.8	3.71	18.94	0.69	5956.39	6705	11.16
PEABODY	65.9	2.77	17.65	0.6	5532.49	6630	16.55
KPU	63.59	2.02	9.32	0.62	5446.66	6619	17.71

In Table 4, the estimated concentration of the elements in coal using the LIBS signal intensity with the SNR method is presented. The estimated calorific value based on the SNR method showed an error range from 10.70 to 22.90% with the calorific value from the chemical analysis. This was quite a large error compared to those of the other methods. In some samples, the carbon and hydrogen concentrations were both underestimated by a maximum of 3%, which made the error larger. Because the SNR method considers the baseline noise in Equation (5), a smoothing method to reduce the effect of random fluctuations may be needed.

Table 4. Predicted calorific value of various coal samples by signal-to-noise ratio method.

Coal Name	Concentration (%)				Calorific Value (kcal/kg)	Chemical Analysis (kcal/kg)	Error
	C	H	O	S			
GUNVOR	73.3	3.77	15.54	0.89	6572.42	7360	10.70
MSJ-1	65.44	3.85	17.98	0.68	5855.07	6915	15.33
MSJ-2	68.75	3.48	20.35	0.79	5895.41	6852	13.96
LANNA HARITA	68.08	3.18	18.18	0.61	5827.31	6619	11.96
MACQUARIE	67.2	2.48	19.46	0.86	5465.48	6705	18.49
PEABODY	63.49	2.18	18.21	0.65	5111.45	6630	22.90
KPU	62.94	2.14	11.12	0.57	5356.83	6619	19.07

5. Conclusions

In order to increase the measurement accuracy of quantitative and qualitative analyses in coal, estimations using the LIBS, the PLS, SNR, and CA methods were performed to validate the measurement accuracy of each method. Based on the estimated concentrations using the CA, PLS, and SNR methods, the calibration curves for each of the elements (C, H, O, and S) were obtained. The calorific values were estimated based on the elemental concentrations of the coal samples acquired from three different analysis methods. The CA method showed an improved accuracy with the R^2 of 0.971 compared to PLS and SNR with R^2 s of 0.914 and 0.777, respectively. The calculated calorific values of coal using Dulong's equation were compared to those of the chemical analysis. The error between the calculated value and the chemical analysis was a minimum of 0.16% to a maximum of 6.99% for the CA method, and those of the PLS and SNR methods ranged from 8.72 to 17.71% and from 10.7 to 22.9%, respectively. The determination of the calorific value using the CA was in good agreement with the value obtained by conventional chemical analysis.

Author Contributions: Conceptualization, S.-M.K. and S.-J.M.; methodology, K.-H.P.; software, K.-H.P.; validation, K.-H.P.; formal analysis, S.-M.K.; investigation, K.-H.P.; data curation, K.-H.P.; funding—acquisition, S.-J.M.; writing—original draft preparation, S.-M.K. and K.-H.P.; writing—review and editing, J.-H.C. and S.-J.M.; visualization, C.-M.R.; supervision, S.-J.M. All authors have read and agreed to the published version of the manuscript.

Funding: This work was supported by the Technology Innovation Program (or Industrial Strategic Technology Development Program—Development of technical support platform for welding material and process) (20017251, Development of laser welding automation system for electric coil joining system to manufacture electrical vehicle motors) funded by the Ministry of Trade, Industry & Energy (MOTIE, Korea).

Data Availability Statement: Not applicable.

Acknowledgments: This work was supported by the National Research Foundation of Korea (NRF) entitled “Development of Coal Analyzing System Using Laser Induced Breakdown Spectroscopy for Clean Coal Power Plant” (No. NRF-2016R1D1A1B03935556). This work was also supported by the Basic Science Research Program through the National Research Foundation (NRF) of Korea entitled “NRF-2016R1D1A1B04934910”.

Conflicts of Interest: The authors declare no conflict of interest. The funders had no role in the design of the study; in the collection, analyses, or interpretation of data; in the writing of the manuscript; or in the decision to publish the results.

References

1. Hwang, Z.W.; Teng, Y.Y.; Li, K.P.; Sneddon, J. Interaction of a laser beam with metals. Part I: Quantitative studies of plasma emission. *Appl. Spectrosc.* **1991**, *45*, 435–441. [[CrossRef](#)]
2. Aguilera, J.A.; Aragon, C.; Campos, J. Determination of carbon content in steel using laser-induced breakdown spectroscopy. *Appl. Spectrosc.* **1992**, *46*, 1382–1387. [[CrossRef](#)]
3. Cremers, D.A.; Radziemski, L.J. Direct detection of beryllium on filters using the laser spark. *Appl. Spectrosc.* **1985**, *39*, 57–63. [[CrossRef](#)]
4. Wachter, J.R.; Cremers, D.A. Determination of uranium in solution using laser-induced breakdown spectroscopy. *Appl. Spectrosc.* **1987**, *41*, 1042–1048. [[CrossRef](#)]
5. Capitelli, F.; Colao, F.; Provenzano, M.R.; Fantoni, R.; Brunetti, G.; Senesi, N. Determination of heavy metals in soils by laser induced breakdown spectroscopy. *Geoderma* **2002**, *106*, 45–62. [[CrossRef](#)]
6. Lazic, V.; Colao, F.; Fantoni, R.; Spizzicchino, V. Laser-induced breakdown spectroscopy in water: Improvement of the detection threshold by signal processing. *Spectrochim. Acta Part B At. Spectrosc.* **2005**, *60*, 1002–1013. [[CrossRef](#)]
7. Gamal, Y.E.D.; Omar, M.M. Study of the electron kinetic processes in laser-induced breakdown of electronegative gases over an extended wavelength range. *Radiat. Phys. Chem.* **2001**, *62*, 361–370. [[CrossRef](#)]
8. Dong, M.; Lu, J.; Yao, S.; Li, J.; Li, J.; Zhong, Z.; Lu, W. Application of LIBS for direct determination of volatile matter content in coal. *J. Anal. At. Spectrom.* **2011**, *26*, 2183–2188. [[CrossRef](#)]
9. Kuzuya, M.; Aranami, H. Analysis of a high-concentration copper in metal alloys by emission spectroscopy of a laser-produced plasma in air at atmospheric pressure. *Spectrochim. Acta Part B At. Spectrosc.* **2000**, *55*, 1423–1430. [[CrossRef](#)]
10. Kuzuya, M.; Murakami, M.; Maruyama, N. Quantitative analysis of ceramics by laser-induced breakdown spectroscopy. *Spectrochim. Acta Part B At. Spectrosc.* **2003**, *58*, 957–965. [[CrossRef](#)]
11. Yuan, T.; Wang, Z.; Lui, S.L.; Fu, Y.; Li, Z.; Liu, J.; Ni, W. Coal property analysis using laser-induced breakdown spectroscopy. *J. Anal. At. Spectrom.* **2013**, *28*, 1045–1053. [[CrossRef](#)]
12. Ismail, M.A.; Imam, H.; Elhassan, A.; Youniss, W.T.; Harith, M.A. LIBS limit of detection and plasma parameters of some elements in two different metallic matrices. *J. Anal. At. Spectrom.* **2004**, *19*, 489–494. [[CrossRef](#)]
13. Li, J.; Lu, J.; Lin, Z.; Gong, S.; Xie, C.; Chang, L.; Li, P. Effects of experimental parameters on elemental analysis of coal by laser-induced breakdown spectroscopy. *Opt. Laser Technol.* **2009**, *41*, 907–913. [[CrossRef](#)]
14. Sivakumar, P.; Taleh, L.; Markushin, Y.; Melikechi, N. Packing density effects on the fluctuations of the emission lines in laser-induced breakdown spectroscopy. *Spectrochim. Acta Part B At. Spectrosc.* **2014**, *92*, 84–89. [[CrossRef](#)]
15. Feng, J.; Wang, Z.; West, L.; Li, Z.; Ni, W. A PLS model based on dominant factor for coal analysis using laser-induced breakdown spectroscopy. *Anal. Bioanal. Chem.* **2011**, *400*, 3261–3271. [[CrossRef](#)]
16. Li, W.; Lu, J.; Dong, M.; Lu, S.; Yu, J.; Li, S.; Liu, J. Quantitative analysis of calorific value of coal based on spectral preprocessing by laser-induced breakdown spectroscopy (LIBS). *Energy Fuels* **2017**, *32*, 24–32. [[CrossRef](#)]
17. Lee, Y.; Choi, D.; Gong, Y.; Nam, S.H.; Nah, C. Laser-induced plasma emission spectra of halogens in the helium gas flow and pulsed jet. *Anal. Sci. Technol.* **2013**, *26*, 235–244. [[CrossRef](#)]
18. Cremers, D.A.; Radziemski, L.J. *Handbook of Laser-Induced Breakdown Spectroscopy*; John Wiley & Sons: Chichester, UK, 2006; pp. 53–58.
19. Gazeli, O.; Stefan, D.; Couris, S. Sulfur detection in soil by laser induced breakdown spectroscopy assisted by multivariate analysis. *Materials* **2021**, *14*, 541. [[CrossRef](#)]
20. Kathiravale, S.; Yunus, M.N.M.; Sopian, K.; Samsuddin, A.H.; Rahman, R.A. Modeling the heating value of municipal solid waste. *Fuel* **2003**, *82*, 1119–1125. [[CrossRef](#)]

21. Lazarek, L.; Antończak, A.J.; Wójcik, M.R.; Drzymała, J.; Abramski, K.M. Evaluation of the laser-induced breakdown spectroscopy technique for determination of the chemical composition of copper concentrates. *Spectrochim. Acta Part B At. Spectrosc.* **2014**, *97*, 74–78. [[CrossRef](#)]
22. Yaroshchik, P.; Death, D.L.; Spencer, S.J. Quantitative measurements of loss on ignition in iron ore using laser-induced breakdown spectroscopy and partial least squares regression analysis. *Appl. Spectrosc.* **2010**, *64*, 1335–1341. [[CrossRef](#)] [[PubMed](#)]
23. Amador-Hernández, J.; García-Ayuso, L.E.; Fernández-Romero, J.M.; de Castro, M.L. Partial least squares regression for problem solving in precious metal analysis by laser induced breakdown spectrometry. *J. Anal. Spectrom.* **2000**, *15*, 587–593. [[CrossRef](#)]
24. Zhang, W.; Zhuo, Z.; Lu, P.; Tang, J.; Tang, H.; Lu, J.; Xing, T.; Wang, Y. LIBS analysis of the ash content, volatile matter, and calorific value in coal by partial least squares regression based on ash classification. *J. Anal. At. Spectrom.* **2020**, *35*, 1621–1631. [[CrossRef](#)]
25. Fisher, B.T.; Johnsen, H.A.; Buckley, S.G.; Hahn, D.W. Temporal gating for the optimization of laser-induced breakdown spectroscopy detection and analysis of toxic metals. *Appl. Spectrosc.* **2001**, *55*, 1312–1319. [[CrossRef](#)]
26. Gornushkin, I.B.; Smith, B.W.; Nasajpour, H.; Winefordner, J.D. Identification of solid materials by correlation analysis using a microscopic laser-induced plasma spectrometer. *Anal. Chem.* **1999**, *71*, 5157–5164. [[CrossRef](#)]